

Low-oxygen freshwaters as ecological niches for mercury methylators

Anthony Kharaillah ^a, Meifang Zhong ^a, Júlia Dordal Soriano ^b, Nicola Gambardella ^c , Isabel Sanz-Sáez ^d , Dongna Yan ^e, Stefan Bertilsson ^f , Erik Björn ^d , Andrea Garcia Bravo ^b , Eric Capo ^{a,*}

^a Department of Ecology, Environment and Geoscience, Umeå University, 90187, Umeå, Sweden

^b Departament de Biología Marina i Oceanografía, Institut de Ciències del Mar, CSIC, Pg Marítim de la Barceloneta 37-49, 08003, Barcelona, Spain

^c Interdisciplinary Centre of Marine and Environmental Research (CIIMAR/CIMAR), University of Porto, Porto, Portugal

^d Department of Chemistry, Umeå University, 90187, Umeå, Sweden

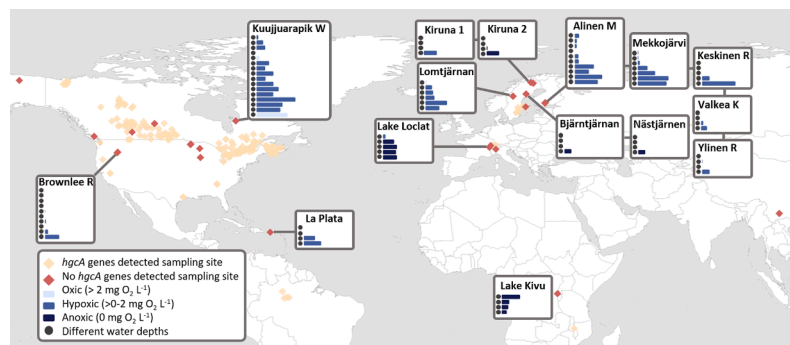
^e State Key Laboratory of Loess Science, Institute of Earth Environment, Chinese Academy of Sciences, Shaanxi Xi'an, 710061, China

^f Department of Aquatic Sciences and Assessment and Science for Life Laboratory, Swedish University of Agricultural Sciences, SE75007, Uppsala, Sweden

HIGHLIGHTS

- Detection of genes involved in mercury methylation in lake water columns.
- Mercury methylation genes more abundant in low-oxygen conditions.
- Desulfobacterota, Bacteroidales and Kirribacteriales are the most abundant mercury methylators in lake water columns.

GRAPHICAL ABSTRACT



ARTICLE INFO

Keywords:
Methylmercury
Metagenomics
Hypoxia/anoxia
Freshwater ecosystems
Climate change

ABSTRACT

Methylmercury (MeHg) is a hazardous neurotoxin, predominantly formed by microbial transformation of inorganic mercury in oxygen-depleted aquatic and terrestrial ecosystems. The ongoing deoxygenation of aquatic ecosystems due to global warming is likely to expand microbial niches for MeHg production. Although mercury methylators have also been reported to thrive in oxygen-deficient conditions in a few marine and freshwater ecosystems, there is a lack of comprehensive understanding of how they are distributed in freshwater systems. In this study, we retrieved *hgcA* genes, genomic marker for mercury methylation potential, from 586 metagenomes from the water column of 186 freshwater systems. Overall, *hgcA* genes were detected in the water column of 30 lakes, with the highest richness and abundance being detected in anoxic (0 mg O₂ L⁻¹) and hypoxic (>0–2 mg O₂ L⁻¹) compared to oxic conditions (>2 mg O₂ L⁻¹). Although Desulfobacterota had the highest *hgcA* gene richness across most freshwater systems, certain systems were dominated by *hgcA* genes from Bacteroidales and Kirribacteriales, implying metabolic and ecological versatility of mercury methylators as a group. Our findings

* Corresponding author.

E-mail address: eric.capo@umu.se (E. Capo).

suggest that projected expanding deoxygenation may lead to new niches for mercury methylators in inland waters.

1. Introduction

The presence of mercury in the environment is a continuous and widespread health hazard with potentially serious consequences for the health of aquatic organisms and humans. Although mercury has always been present in ecosystems due to natural processes such as weathering and volcanic eruptions, anthropogenic emissions resulting from e.g., cement production and fossil fuel combustion (Pirrone et al., 2010) have increased mercury concentrations in the environment by more than threefold (Mason et al., 2012). While anthropogenic emissions have been reduced in the Northern Hemisphere, mercury is still circulating in food webs and ecosystems as it is only slowly sequestered. Thus, mercury is classified as a 'ubiquitous, persistent, bioaccumulative and toxic' substance, particularly in its methylated form (MeHg). MeHg is a potent neurotoxin that can bypass the blood-brain barrier and accumulate in the central nervous system (Aschner and Aschner, 1990), exacerbating harmful effects that manifest as neurological and cardiovascular symptoms (Choi et al., 2009). The presence of MeHg in the environment is mainly driven by the transformation of inorganic mercury into MeHg by microorganisms that carry two genes involved in mercury methylation: *hgcA* and *hgcB* (Parks et al., 2013). As the amino acid sequences of the proteins coded from these genes contain highly conserved regions, it is possible to identify mercury methylators from the detection of those genes directly in environmental DNA samples. This approach has been widely adopted to determine the diversity and prevalence of mercury methylators in different ecosystems (Podar et al., 2015; Gionfriddo et al., 2020; Capo et al., 2023a).

Mercury methylation is well known to occur in a wide range of aquatic ecosystems (Bravo and Cosio, 2020); however, there are few studies assessing the distribution of mercury methylators in the water columns of these ecosystems through omics approaches (i.e., metagenomics, metabarcoding), making it difficult to determine how environmental conditions relate to the presence of mercury methylators. While many mercury methylators have been identified in coastal waters and sediments (Lin et al., 2021; Capo et al., 2022a), only a few lake ecosystems have been studied in this regard (Jones et al., 2019; Peterson et al., 2020; BD 2023; Gallorini and Loizeau, 2022; Capo et al., 2023b; Gambardella et al., 2025). Lakes, being highly variable in typology, hydrological dynamics, and biodiversity, are excellent study objects to gain a comprehensive understanding of how environmental factors shape mercury-methylating communities. In mono-, di-, and polymictic lakes, surface and deep waters mix once, twice, or multiple times per year due to the difference in density between upper and lower waters (i.e., thermal mixing). This creates strong and dynamic chemical gradients as oxygen and nutrients (from sediments) are imported to hypoxic and anoxic water masses (Woolway et al., 2020). With current global increases in land, air, and water temperatures, hypoxic and anoxic conditions are predicted (and have been shown) to increase in freshwater systems due to lower oxygen solubility (Jane et al., 2021; Zhang et al., 2025) and induced thermal stratification of water columns. Additionally, enhanced primary production and algal blooms – fuelled by climate warming and eutrophication – contribute to the depletion of oxygen (Friedrich et al., 2014). Bacterial decomposition of decaying algae (Hintemann, 2010) leads to the formation of so-called 'dead zones' that can continuously promote algal blooms due to nutrient (i.e., phosphorus) cycling from sediments back up towards the epilimnion (Zou et al., 2020). Altogether these environmental changes are expected to augment niches for mercury methylators, known to transform mercury into MeHg in oxygen-deficient conditions as reported from both incubation experiments (Pereira-Garcia et al., 2025) and long-term environmental records (Zhong et al., 2025).

In this project, we analyzed 586 publicly available metagenomes from a total of 186 freshwater systems (lakes, ponds and reservoirs) mostly located in the Northern Hemisphere, using the bioinformatic pipeline marky-coco (Capo et al., 2023a) to detect and quantify *hgcA* genes from water columns. This enabled us to (i) investigate the presence of mercury methylators in the water columns of freshwater systems, (ii) assess the impact of oxygen availability in controlling the presence and abundance of potential mercury methylators, and (iii) explore biogeographic distribution patterns of mercury methylators in a variety of freshwater ecosystems.

2. Material and methods

2.1. Dataset

The dataset compiled in this study (Table 1) contained metagenomes from the water column across 186 freshwater systems (lakes, ponds, reservoirs) distributed worldwide with predominant representation from the Northern Hemisphere. For each sample, the raw sequencing data obtained were associated with metadata containing a compilation of environmental parameters including depth (m), dissolved oxygen concentrations (mg O₂L⁻¹), temperature (°C), pH, nutrient concentrations and other physicochemical characteristics (Datasheet 1A).

2.2. Bioinformatics

The detection, counting and taxonomic identification of *hgcA* genes from metagenomes was done using the pipeline marky-coco (Capo et al., 2023a). The metagenomes were trimmed and cleaned using fastp (Chen et al., 2018) with the following parameters:q 30 -l 25 -detect_adapter_for_pe -trim_poly_g -trim_poly_x. A de novo single assembly approach was applied using the assembler megahit 1.1.2 (Li et al., 2015) with default settings. Then, microbial community composition was determined using the software MetaPhlan2 v4.1.1 (Truong et al., 2015) (Datasheet 1B). The annotation of contigs for prokaryotic protein-coding gene prediction was done with the software prodigal v2.6.3 (Hyatt et al., 2010). The DNA reads were mapped against the contigs with bowtie2 (Langmead and Salzberg, 2012), and the resulting .sam files were converted to .bam files using samtools 1.9 (Li et al., 2009). The .bam files and the prodigal output .gff file were used to estimate read counts by using featureCounts (Liao et al., 2014). To detect *hgcA* genes, we used the procedure described in Capo et al. (2023a).

Table 1

Dataset of metagenomes used in the present study. Detailed information is provided in Datasheet 1A.

References	#freshwater systems	#metagenomes	Location
BD Peterson et al. (2023)	1	33	Brownlee Reservoir (US)
Capo et al. (2023b)	1	11	Lake Geneva (France-Switzerland)
Garner et al. (2023)	160	160	Canada
Sanseverino et al. (2022)	1	24	Lake Varese (Italy)
Buck et al. (2021)	38	258	Worldwide
Jones et al. (2019)	2	5	Lake Manganika & McQuade (US)
Peterson et al. (2020)	1	5	Lake Mendota (US)
Xing et al. (2020)	1	5	Lake Fuxian (China)
Yang et al. (2019)	23	57	Worldwide

HMM profiles from the Hg-MATE database (v1) were applied to the amino acid FASTA file generated from each assembly with the function *hmmsearch* from HMMER v3.2.1 (Finn et al., 2011). Genes with E-values $<10^{-3}$ were considered as significant hits. To further confirm putative *hgcA* genes within the HMM search hits, we used the high stringency cutoff defined by Capo et al. (2023a) by screening *hgcA* homologs for 6 amino acids with the following motifs: NVWCAAGK, NVWCASGK, NVWCAGGK, NIWCAGGK, NIWCAGGK or NVWCSAGK.

Coverage values of *hgcA* genes were calculated as the number of reads mapped to the gene divided by its length in base pairs and were further normalized by dividing them by the summed coverage values of the single copy gene *rpoB* (both bacteria and archaea together) (Datasheet 1C). The *rpoB* genes were detected using the HMM profile TIGR02013.hmm and TGR03670.hmm for bacterial and archaeal *rpoB* genes, respectively, and applying the trusted cutoff provided in HMM files. The reference package 'hgcA' from Hg-MATE.db.v1 was used for phylogenetic analysis of the HgcA amino acid sequences. Briefly, amino acid sequences from a gene identified as *hgcA* gene homolog were (i) compiled in a FASTA file, (ii) aligned to Stockholm formatted alignment of *hgcA* sequences from the reference package with the function *hmmalign* from HMMER (iii) placed onto the HgcA reference tree with the function *pplacer* and (iv) classified using the functions *rppr* and *guppy_classify* from the program *pplacer* v1.1.alpha19 (Matsen et al., 2010). A taxonomic identifier (NCBI txid) was therefore assigned to each gene and used to create an *hgcA*⁺ taxa abundance table for downstream statistical analysis (Datasheet 1D).

2.3. Data analysis

Data analysis was conducted in R version 4.3.3 (2023–10–31 ucrt) (R Core Team, 2023). A map was done using the package *rnaturrearth* v1.0.1 (South and South, 2017) (Datasheet 1E), barplots and the dotplot using the package *ggplot2* v3.5.2 (Wickham, 2011) and the PCoA analysis was performed using the function *ordinate* from *phyloseq* v1.46.0 (McMurdie and Holmes, 2013). A Kruskal–Wallis test pairwise comparisons were performed using Dunn's test with Benjamini–Hochberg correction (*dunnTest()* from the *FSA* package v0.10.0 (Ogle and Ogle, 2017)). To investigate the relationships between *hgcA* gene distribution and oxygen concentrations, samples were categorized into four categories: oxic ($\geq 2 \text{ mg O}_2 \text{ L}^{-1}$), hypoxic ($>0\text{--}2 \text{ mg O}_2 \text{ L}^{-1}$) and anoxic ($0 \text{ mg O}_2 \text{ L}^{-1}$), and samples with no measured oxygen concentrations (Jürgens and Taylor, 2018). The ANOSIM analysis was performed by using the *anosim* function in *vegan* v2.6–10 (Oksanen et al., 2013). Pearson correlation coefficients were calculated to assess linear relationships between *hgcA* gene abundance and the environmental parameters that have $<60\%$ of "na"s values (Datasheet 1F) i.e., Pearson correlation coefficients were then computed on the filtered dataset and visualized as a heatmap using the *corrplot* package in R (Wei and Simko, 2021) and *hmisc* R package (Harrell and Harrell, 2019). The *TITAN2* package v2.4.2 (Baker and King, 2010) was used to detect changes in *hgcA*⁺ taxa distributions along an oxygen gradient over the lakes that found *hgcA* genes, and assess synchrony among taxa change points as evidence for community thresholds. Taxa that occurred in <3 metagenomes (27 txid) were excluded to ensure robust indicator selection. Then, indicator species z scores (rescaled "IndVal" score) (Dufrêne and Legendre, 1997; Baker and King, 2010) were calculated to integrate occurrence, abundance and directionality of taxa responses by using *TITAN2* default settings (minSplt = 5, numPerm = 2, nBoot = 500, pur. cut = 0.95, etc.). Other packages that assisted in the above analysis and illustration include: *dplyr* v1.1.4 (Wickham et al., 2024), *tidy* v1.3.1 (Wickham et al., 2024), *viridis* v0.6.5 (Garnier et al., 2024), *packcircles* v0.3.7 (Bedward et al., 2024), *ggforce* v0.4.2 (Pedersen, 2023), *scales* v1.4.0 (Wickham et al., 2016) and *gchicklet* v0.5.2 (Rudis and Bichat, 2023).

3. Results

A total of 2294 *hgcA* genes were detected in the water columns across 30 of the 186 studied freshwater systems, corresponding to 217 metagenomes out of the total 586 analyzed (Graphical abstract, Fig. S1, Datasheet 1A). From metagenomes where *hgcA* genes were detected, the *hgcA* gene abundance (*hgcA* coverage values normalized by *rpoB* coverage values) ranged from 0.0003 – 0.4339 (Datasheet 1C). The *hgcA* genes were taxonomically assigned to 119 microbial taxa (NCBI txid, different taxonomic levels from phylum to genus) with the highest diversity observed for *Desulfobacterota* (39), *Firmicutes* (14), *Euryarchaeota* (11), *Chloroflexota* (8) and *Spirochaetes* (8) (Datasheet 1D). The composition of *hgcA* assemblages differed between the 30 freshwater systems (Fig. 1, Fig. S1). At the order level, certain taxa appeared to be broadly prevalent i.e., *Kirimatiellales* (txid2026799, detected in 23 systems) and *Bacteroidales* (txid171549, 22 systems). At the genus level, *Syntrophus* (txid2676650) and *Methanoregula* (txid2052170) were both detected in 13 systems. A high number of txids were found in <15 lakes i.e., *Bacteroidetes* (txid976, 14 systems), *BSN033* (txid122706, 7 systems) and *Desulfovibrio* (txid2593640, 6 samples from Ainen Mustajarvi) were only detected in a single lake. Overall, some freshwater systems i.e., Ainen Mustajarvi, Kuujjuarapik-Whapmagoosti and Mekkojarvi exhibited higher *hgcA* richness and abundance, compared to other systems.

Most *hgcA* genes were found in metagenomes obtained from hypoxic (128) and anoxic (27) samples compared to oxic samples (17) (45 samples had no oxygen data available) (Datasheet 1E). Additionally, the average relative abundance of *hgcA* genes was higher in hypoxic-anoxic samples with significant differences observed between oxic and hypoxic-anoxic samples (Kruskal–Wallis post-hoc tests, $p < 0.001$) but not between hypoxic and anoxic samples ($p = 0.08$) (Fig. 2). Overall, a Pearson correlation analysis showed that *hgcA* gene abundance was significantly and negatively correlated with oxygen concentrations, temperature and pH and negatively to ammonium concentrations (Fig. S2). In terms of community structure, a PCoA analysis showed that both the broader prokaryotic communities (Fig. 3A) and the *hgcA* assemblages (Fig. 3B) were similar within the same lake, although some intra-lake heterogeneity could be observed in e.g., Lake Loclat. ANOSIM analysis showed statistical differences of both the structure of the prokaryotic community and *hgcA* assemblage based on oxygen categories (ANOSIM, $p < 0.001$), as illustrated by ellipsoids in the PCoA plots. The prokaryotic community structure showed significant separation between anoxic and hypoxic ($p < 0.001$), as well as hypoxic and oxic ($p < 0.001$), but no significant difference was detected between anoxic and oxic samples ($p = 0.296$). In contrast, the *hgcA* assemblages in anoxic and hypoxic samples were significantly different from each other ($p < 0.001$) while a less marked difference was found for anoxic and oxic ($p = 0.045$) and there were no significant differences between hypoxic and oxic samples ($p = 0.117$).

A TITAN2 analysis was used to detect the presence of microbial taxa that serve as indicators of shifts in *hgcA* assemblage structure along the oxygen gradient (Fig. 4, Fig. S3). Based on the 0.95 thresholds chosen for purity and reliability parameters, 15 out of 119 taxa were deemed to be statistically pure and reliable indicators. Among them, 13 were considered to have decreasing *hgcA* abundance (z-) with dissolved oxygen increases. Most of these indicator taxa exhibited pronounced decreases in *hgcA* abundance with increasing oxygen concentrations around 0.1 to 0.4 mg O₂ L⁻¹ such as *Actinobacteria* (txid1883427) and *Geobacterales* (txid213422). Among them, two indicator taxa showed decreased abundance in *hgcA* with increasing oxygen ($>0 \text{ mg O}_2 \text{ L}^{-1}$), i.e., *Aminicenantes* (txid910038) and *Syntrophales* (txid213463). In contrast, *Methanoregula* (txid2649730) and *Desulfovibrio* (txid213121), exhibited stronger and more consistent increases in *hgcA*

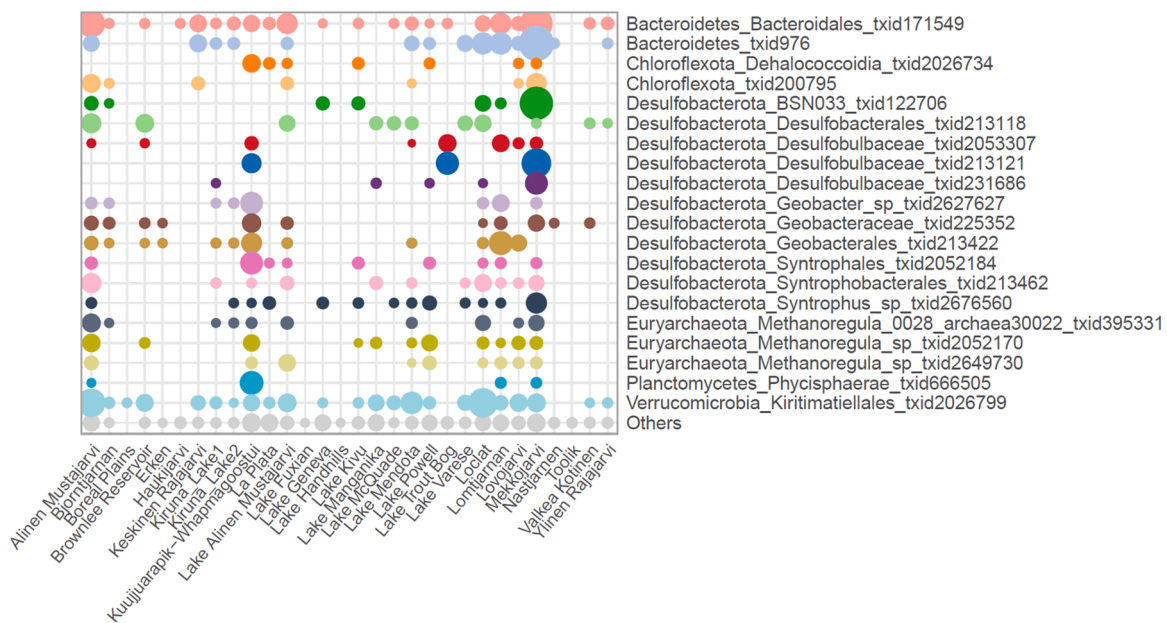


Fig. 1. Heatmap showing the *hgcA* abundance of each txid in the 30 lakes where *hgcA* genes were found.

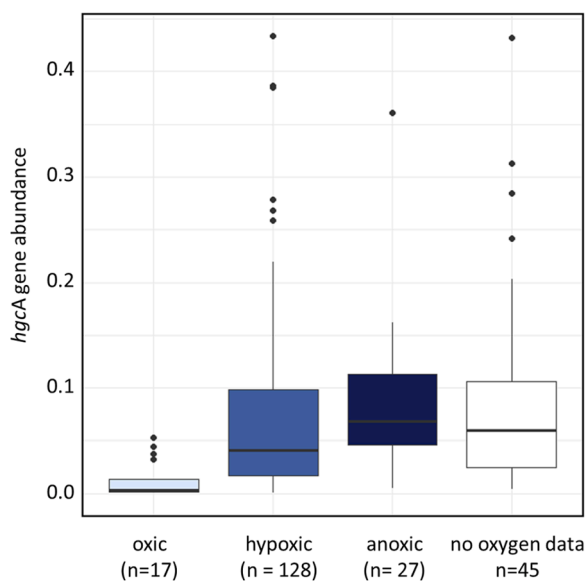


Fig. 2. Boxplot displaying the *hgcA* abundance from each metagenome with different oxygen concentrations: light blue for oxic ($\geq 2 \text{ mg O}_2 \text{ L}^{-1}$), blue for hypoxic ($0.2-2 \text{ mg O}_2 \text{ L}^{-1}$) and dark blue for anoxic ($0 \text{ mg O}_2 \text{ L}^{-1}$). The number of samples considered for each category is displayed in the figure (n values).

abundance ($z+$) along the oxygen gradient with peaked $z+$ values found at 0.55 and 0.4 $\text{mg O}_2 \text{ L}^{-1}$, respectively.

4. Discussion

Oxygen is a critical controlling factor for mercury methylation, but its effects on the diversity and ecology of mercury-methylating micro-organisms remain poorly understood (Cabrol et al., 2023). Previous studies have investigated the relationship between *hgcA* abundance and oxygen levels (Capo et al., 2022a; Ji et al., 2020a, 2020b). Generally, an increase in oxygen is paralleled by a decrease in *hgcA* abundance. This inverse correlation between oxygen and *hgcA* has proven so strong that some successful mitigation strategies have implemented oxygen nanobubbles to reduce *hgcA* abundance and mercury bioavailability (Ji et al.,

2020a, 2020b). Interestingly, some evidence of aerobic mercury methylation has been reported leading researchers to hypothesise the existence of other metabolic pathways for aerobic mercury methylation (Cao et al., 2021).

The dataset compiled in this study encompasses environmental genomic data from both systems previously unexplored for mercury cycling (Yang et al., 2019; Buck et al., 2021; Garner et al., 2023) and environments where mercury methylators have been the focus (Jones et al., 2019; Peterson et al., 2020; BD 2023). Noticeably, most freshwater systems from which metagenomic data could be collected were located in socially developed regions as a consequence of the inequities in global lake science (Jiang et al., 2025). A systematic re-analysis of all metagenomes from these systems with the consensus protocol developed by Capo et al. (2023b) allows for an unbiased comparison of the diversity and prevalence of mercury methylators across a large collection of metagenomes from various freshwater bodies, as well as statistically sound assessments of relationships between oxygen conditions and the abundance of *hgcA* genes, the genetic marker for mercury methylation. It has been showed that the abundance and expression of *hgcA* genes in the environment do not necessarily correlate for all mercury methylation (e.g., Capo et al., 2022b), precluding the use *hgcA* abundance estimates from metagenomes as direct evidence of mercury methylation on ecosystems.

4.1. Prevalence of mercury methylators in freshwater ecosystems

Prior to the discovery of the *hgcAB* gene pair (Parks et al., 2013), the vast majority of mercury methylators, cultivated and tested in laboratory experiments (Gilmour et al., 2013), were identified as Desulfobacterota (previously referred to as Deltaproteobacteria), Firmicutes (including Clostridia), and Euryarchaeota (Methanobacteria). Most of the recent molecular studies looking for *hgcA* genes from environmental genomic datasets revealed that Desulfobacterota accounted for most of the taxa in mercury-methylating assemblages (Capo et al., 2022a; Peterson et al., 2020). They are also occasionally predominant in terms of *hgcA* gene abundance, with pertinent examples from the water column of the Baltic Sea (Capo et al., 2022a), Black Sea (Cabrol et al., 2023) and thermokarst lakes (Gambardella et al., 2025). In the present study focusing on freshwater ecosystems, Desulfobacterota featured the largest *hgcA* richness with 39 microbial taxa (from genus to phylum) and was dominant in most systems e.g., Mekkojärvi, Lake TroutBog,

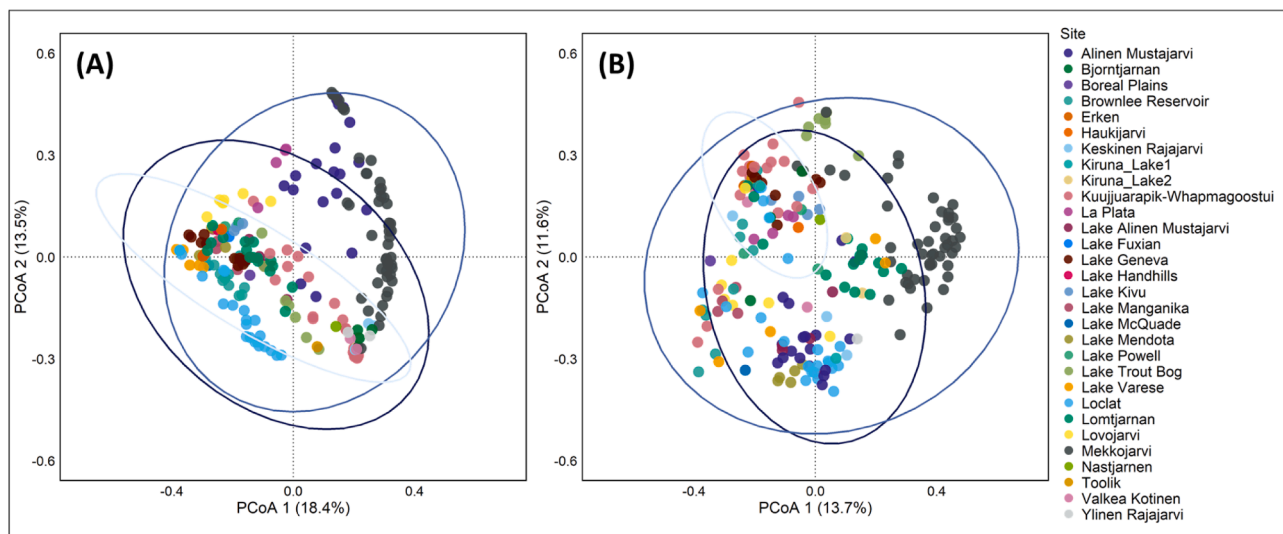


Fig. 3. PCoA plots showing Bray-Curtis dissimilarity values of the whole prokaryotic community (A) and of *hgcA* assemblages (B). Ellipsoids depicted the oxygen categories associated with each sample: light blue for oxic ($\geq 2 \text{ mg O}_2 \text{ L}^{-1}$), blue for hypoxic ($>0-2 \text{ mg O}_2 \text{ L}^{-1}$) and dark blue for anoxic ($0 \text{ mg O}_2 \text{ L}^{-1}$).

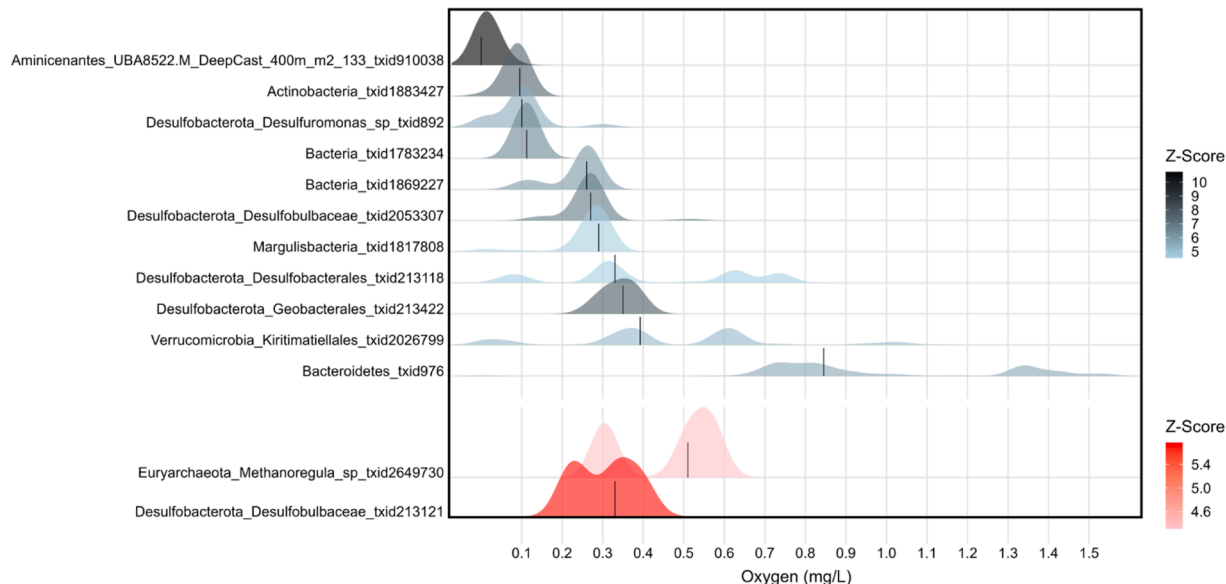


Fig. 4. TITAN2 analysis. TITAN2 analysis linking *hgcA* txid abundance to an oxygen gradient. Each point represents a txid, with its position along the x-axis indicating its change point (i.e., the point along the oxygen gradient where its abundance shifts most strongly), and the y-axis showing the strength and direction of the response (positive or negative). Significant taxa identified as indicators of increasing (red colors) or decreasing (dark colors) oxygen are highlighted.

Lomtjärnan, Kuujjuarapik-Whapmagoostui (Fig. 1). However, they were not predominant in the majority of the freshwater systems analyzed e.g., Lake Ainen Mustajärvi or Lake Loclat dominated by Kiritimatiellales and Bacteroidales. In agreement with Jones et al. (2019), our re-analysis of water metagenomes from the hypereutrophic sulfidic Lake Manganika and mesotrophic McQuade revealed that Aminicenantes (txid910038), Spirochaetes (txid1130380) and Kiritimatiellales (txid2026799) were the taxa with the highest *hgcA* abundance. In the sulfate-enriched eutrophic Lake Mendota (Minnesota, USA), Kiritimatiellaeota and Bacteroidetes were the dominant mercury methylators while Desulfobacterota accounted only for 22 % of the *hgcA* genes (Peterson et al., 2020). The re-analysis of Peterson et al.'s (2020) metagenomic data with the updated Hg-MATE database confirmed the previously found pattern with dominant microbial taxa in Lake Mendota water columns being txid2026799 (Kiritimatiellales) and txid171549 (Bacteroidales) (Fig. S1). In Lake Geneva, predominant *hgcA* genes were

identified as Firmicutes from sediment trap samples (Capo et al., 2023b), further annotated as Clostridiales in the present study (txid31979, txid186802) (Datasheet 1C). Moreover, the high *hgcA* richness found in Kuujjuarapik-Whapmagoostui aligned with recent findings in such areas, making this region a point of interest for the study of mercury methylation in the Arctic (Gambardella et al., 2025). Altogether, the findings of our meta-analysis illustrate the high diversity of mercury methylators, many of which remain poorly understood in terms of their ecology.

4.2. Mercury methylators thrive in low-oxygen conditions in freshwater systems

Mercury methylators convert inorganic mercury into MeHg under anaerobic conditions (Bravo and Cosio, 2020), with the highest methylation rates hypothesized to occur in anoxic conditions, including

anoxic water columns (Capo et al., 2022a; Eckley and Hintelmann, 2006; Hintelmann, 2010). Consistently, *hgcA* genes are predominantly found in water columns with hypoxic and anoxic/euxinic conditions such as the Black Sea (Cabrol et al., 2023), the Baltic Sea (Capo et al., 2022a), the Saanich Inlet (Lin et al., 2021) and Lake Mendota (Peterson et al., 2020). Our meta-analysis revealed that *hgcA* genes were predominantly found in anoxic ($0 \text{ mg O}_2 \text{ L}^{-1}$) and hypoxic ($>0\text{--}2 \text{ mg O}_2 \text{ L}^{-1}$) conditions, with only a slightly higher abundance in anoxic environments. Previous studies have studied the links between *hgcA* gene abundance and MeHg concentrations and mercury methylation rates in lake water columns (Jones et al., 2019; Peterson et al., 2020; BD 2023) but there is only a few studies highlighting such links in oxygen deficient environments.

In our meta-analysis, we found a clear pattern showing that *hgcA* genes are more abundant in anoxic than hypoxic or in oxic conditions (Fig. 3) and that *hgcA* assemblages are also clustered according to prevailing oxygen levels (Fig. 4, ANOSIM analysis). Sulfate-reducing bacteria, iron-reducing bacteria, and methanogens were the most commonly reported mercury methylators (Fleming et al., 2006; Gilmour et al., 2013), all of them being known to respire without oxygen via anaerobic respiration. However, more recent studies revealed the versatility of mercury methylators including potential capability for microaerophily or syntrophy (McDaniel et al., 2020; Lin et al., 2021; Vigneron et al., 2021) open discussions about the relationships between oxic conditions and mercury methylation. In our study, the TITAN2 analysis identified 15 out of 119 microbial taxa as statistically significant indicators of community shifts along the dissolved oxygen gradient (Fig. 4). Of these, 13 taxa exhibited negative z-scores ($z-$), indicating a significant decline in *hgcA*-associated abundance with increasing oxygen concentrations. This suggests a preference for suboxic or anoxic conditions. In contrast, two taxa—*Methanoregula* (txid2649730) and a representative of the Desulfobulbaceae family (txid213121)—displayed positive z-scores ($z+$), representing increasing abundance with higher (but still hypoxic) oxygen levels. Although *Methanoregula* is known as an anaerobic methanogen, a recent study revealed its presence in oxic waters (Kallistova et al., 2023). Breakpoints for each responsive taxon were distributed across the lower-to-intermediate range of the oxygen gradient, highlighting the transitional zone as a hotspot for community turnover of the mercury-methylating assemblage. All the taxa identified as potential indicators of community shifts are microorganisms that are typically favored by oxygen-deficient conditions. As metabolic capacities of microorganisms can vary even within families, it is difficult to provide robust inferences about their actual metabolic roles in these ecosystems.

Considering that oxic environments preferentially select for microorganisms that use oxygen as their predominant electron acceptor (with higher energy yield), mercury methylators are not expected to be found in such water masses. However, it has been shown that *hgcA* genes can be found in sediment traps underlying the oxic water column of Lake Geneva (Capo et al., 2023b) where relatively high MeHg concentrations and significant mercury methylation rates were previously observed (Gascón Díez et al., 2016). In the oxic water column, mercury methylators would have the potential to persist and grow in anaerobic microhabitats such as sinking particles (Bianchi et al., 2018; Gallorini and Loizeau, 2021; 2022), animal guts (Gorokhova et al., 2020) or periphyton (Cleckner et al. 1999). However, *hgcA* genes are rarely detected directly in oxic water samples using metagenomic data. In the present study, 17 metagenomes in which *hgcA* genes were detected had oxic conditions ($\geq 2 \text{ mg O}_2 \text{ L}^{-1}$). Noticeably, most oxygen values were below fully oxic conditions (range $2.18\text{--}9.02 \text{ mg O}_2 \text{ L}^{-1}$, mean = 6.40 , $sd = 2.20$), potentially explaining the detection of putative mercury methylators in conditions defined as oxic, while these environments may in fact represent the redox transition zone or sinking/suspended particles.

5. Conclusions

Our study identified the presence of *hgcA* genes in specific lakes, indicating potential hotspots for methylmercury production. Specifically, low-oxygen – both hypoxic and anoxic – water layers appear to be favorable ecological niches for *hgcA*⁺ microorganisms with inter-lake differences in the taxonomy of mercury-methylating groups. These findings suggest that certain freshwater systems may be particularly vulnerable to mercury methylation, especially as climate change and enhanced deoxygenation the likelihood of low-oxygen water layers— even within water layers that are currently oxic. This underscores the need for closer monitoring of these ecosystems and provides a valuable resource for informing lake management strategies and guiding fish consumption advisories to protect both environmental and human health.

Supplementary information

Datasheet 1. This datasheet includes the following information (A) List of metagenomic data with related metadata (sequencing run, bioinformatics metrics, environmental parameters and associated references) (B) Outputs of the metaphlan analysis showing the community composition signal obtained for each metagenome (C) The *hgcA* gene abundance table showing information about the gene abundance, normalization and taxonomu (D) The *hgcA* gene abundance table at the txid level (NCBI taxonomic identifier) (E) Table used for the map generated in the Graphical abstract (F) Table used for the Pearson correlation analysis.

Figure S1. Composition barplots of the *hgcA* assemblages for each of the 30 lakes where *hgcA* genes were found. Oxygen concentrations are depicted by the colors of the id of each metagenome with the following color code: light blue for oxic ($\geq 2 \text{ mg O}_2 \text{ L}^{-1}$), blue for hypoxic ($0\text{--}2 \text{ mg O}_2 \text{ L}^{-1}$) and dark blue for anoxic ($0 \text{ mg O}_2 \text{ L}^{-1}$).

Figure S2. Pearson correlation heatmap of environmental parameters, *hgcA* gene abundance and number of DNA reads (cleaned reads). See Datasheet 1A for further information about environmental parameters and how they were obtained for each sample.

Figure S3. Community-level TITAN2 analysis showing indicator response strength along an oxygen gradient. The solid blue and red lines represent the cumulative sum of standardized z-scores (fsumz⁺ for positive responders and fsumz⁻ for negative responders, respectively), indicating the aggregated strength of taxa responses increasing or decreasing with oxygen. Shaded areas or density curves depict the distribution of individual taxa change points. The filtered sum(z) curve highlights zones of significant community response, where indicator taxa exhibit consistent directional change along the gradient.

Funding information

EC was funded by the Swedish Research Council VR (VR starting grant 2023-03,504), Gustafssons stiftelser (2508) and the Climate Impacts Research Centre. The computations were enabled by resources provided by the National Academic Infrastructure for Supercomputing in Sweden (NAIIS), partially funded by the Swedish Research Council through grant agreement no 2023/5-183, 2024/5-194 and 2023/6-139, 2024/6-110.

CRediT authorship contribution statement

Anthony Kharailah: Writing – original draft, Visualization, Validation, Methodology, Formal analysis. **Meifang Zhong:** Writing – original draft, Visualization, Validation, Supervision, Formal analysis. **Júlia Dordal Soriano:** Writing – review & editing, Formal analysis. **Nicola Gambardella:** Writing – review & editing, Methodology, Investigation. **Isabel Sanz-Sáez:** Writing – review & editing, Methodology, Investigation, Formal analysis. **Dongna Yan:** Writing – review &

editing, Methodology. **Stefan Bertilsson**: Writing – review & editing, Methodology, Investigation, Conceptualization. **Erik Björn**: Writing – review & editing, Methodology, Investigation, Conceptualization. **Andrea Garcia Bravo**: Writing – review & editing, Methodology, Investigation, Conceptualization. **Eric Capo**: Writing – review & editing, Writing – original draft, Visualization, Validation, Supervision, Software, Resources, Project administration, Methodology, Investigation, Funding acquisition, Formal analysis, Data curation, Conceptualization.

Declaration of competing interest

There is not competing interest.

Supplementary materials

Supplementary material associated with this article can be found, in the online version, at [doi:10.1016/j.watres.2025.125014](https://doi.org/10.1016/j.watres.2025.125014).

Data availability

Data link is provided in the Supplementary Information Datasheet.

References

Aschner, M., Aschner, J.L., 1990. Mercury neurotoxicity: mechanisms of blood-brain barrier transport. *Neurosci. Biobehav. Rev.* 14 (2), 169–176. [https://doi.org/10.1016/S0149-7634\(05\)80217-9](https://doi.org/10.1016/S0149-7634(05)80217-9).

Baker, M.E., King, R.S., 2010. A new method for detecting and interpreting biodiversity and ecological community thresholds. *Methods Ecol. Evol.* 1 (1), 25–37. <https://doi.org/10.1111/j.2041-210X.2009.00007.x>.

Bedward, Eppstein, D., Menzel, P., 2024. packcircles: circle Packing, R package version 0.3.7. <https://CRAN.R-project.org/package=packcircles>.

Bravo, A.G., Cosio, C., 2020. Biotic formation of methylmercury: a bio-physico-chemical conundrum. *Limnol. Ocean.* 65 (5), 1010–1027. <https://doi.org/10.1002/lno.11366>.

Bianchi, D., Weber, T.S., Kiko, R., Deutsch, C., 2018. Global niche of marine anaerobic metabolisms expanded by particle microenvironments. *Nat. Geosci.* 11 (4), 263–268. <https://doi.org/10.1038/s41561-018-0081-0>.

Buck, M., García, S.L., Fernandez, L., Martin, G., Martinez-Rodriguez, G.A., Saarenheimo, J., Zopfi, J., Bertilsson, S., Peura, S., 2021. Comprehensive dataset of shotgun metagenomes from oxygen stratified freshwater lakes and ponds. *Sci Data* 8 (1), 131. <https://doi.org/10.1038/s41597-021-00910-1>.

Cao, D., Chen, W., Xiang, Y., Mi, Q., Liu, H., Feng, P., Shen, H., Zhang, C., Wang, Y., Wang, D., 2021. The efficiencies of inorganic mercury bio-methylation by aerobic bacteria under different oxygen concentrations. *Ecotoxicol. Env. Saf.* 207, 111538. <https://doi.org/10.1016/j.ecoenv.2020.111538>.

Cabrol, L., Capo, E., van Vliet, D.M., von Meijenfeldt, F.A.B., Bertilsson, S., Villanueva, L., Sánchez-Andrea, I., Björn, E., Bravo, A., Heimbürger Boavida, L-E., 2023. Redox gradient shapes the abundance and diversity of mercury-methylating microorganisms along the water column of the Black Sea. *mSystems* 8 (4). [https://doi.org/10.1128/msystems.00537-23 e00537-23](https://doi.org/10.1128/msystems.00537-23).

Capo, E., Feng, C., Bravo, A.G., Bertilsson, S., Soerensen, A.L., Pinhassi, J., Buck, M., Karlsson, C., Hawkes, J., Björn, E., 2022a. Expression levels of hgcAB genes and mercury availability jointly explain methylmercury formation in stratified brackish waters. *Env. Sci. Technol.* 56 (18), 13119–13130. <https://doi.org/10.1021/acs.est.2c03784>.

Capo, E., Broman, E., Bonaglia, S., Bravo, A.G., Bertilsson, S., Soerensen, A.L., Pinhassi, J., Lundin, D., Buck, M., Hall, P.O.J., Nascimento, F.J.A., Björn, E., 2022b. Oxygen-deficient water zones in the Baltic Sea promote uncharacterized Hg methylating microorganisms in underlying sediments. *Limnol. Ocean.* 67 (1), 135–146. <https://doi.org/10.1002/lno.11981>.

Capo, E., Peterson, B.D., Kim, M., Jones, D.S., Acinas, S.G., Amyot, M., Bertilsson, S., Björn, E., Buck, M., Cosio, C., Elias, D.A., Gilmour, C., Goni-Urriza, M., Gu, B., Lin, H., Liu, Y.-R., McMahon, K., Moreau, J.W., Pinhassi, J., Podar, M., Puent-Sánchez, F., Sánchez, P., Storck, V., Tada, Y., Vignerón, A., Walsh, D.A., Vandewalle-Capo, M., Bravo, A.G., Gionfriddo, C.M., 2023a. A consensus protocol for the recovery of mercury methylation genes from metagenomes. *Mol. Ecol. Resour.* 23 (1), 190–204. <https://doi.org/10.1111/1755-0998.13687>.

Capo, E., Cosio, C., Gascón Díez, E., Loizeau, J.-L., Mendes, E., Adatte, T., Franzenburg, S., Bravo, A.G., 2023b. Anaerobic mercury methylators inhabit sinking particles of oxic water columns. *Water Res.* 229, 119368. <https://doi.org/10.1016/j.watres.2022.119368>.

Chen, S., Zhou, Y., Chen, Y., Gu, J., 2018. fastp: an ultra-fast all-in-one FASTQ preprocessor. *Bioinformatics* 34 (17), i884–i890. <https://doi.org/10.1093/bioinformatics/bty560>.

Choi, A.L., Weihe, P., Budtz-Jørgensen, E., Jørgensen, P.J., Salonen, J.T., Tuomainen, T.-P., Murata, K., Nielsen, H.P., Petersen, M.S., Askham, J., Grandjean, P., 2009. Methylmercury exposure and adverse cardiovascular effects in Faroese whaling men. *Env. Health Perspect* 117 (3), 367–372. <https://doi.org/10.1289/ehp.11608>.

Cleckner, L.B., Gilmour, C.C., Hurley, J.P., Krabbenhoft, D.P., 1999. Mercury methylation in periphyton of the Florida Everglades. *Limnol. Ocean.* 44 (7), 1815–1825. <https://doi.org/10.4319/lo.1999.44.7.1815>.

Dufrêne, M., Legendre, P., 1997. Species assemblages and indicator Species: the need for a flexible asymmetrical approach. *Ecol. Monogr.* 67 (3), 345–366. [https://doi.org/10.1890/0012-9615\(1997\)067\[0345:SAAIST\]2.0.CO;2](https://doi.org/10.1890/0012-9615(1997)067[0345:SAAIST]2.0.CO;2).

Eckley, C.S., Hintelmann, H., 2006. Determination of mercury methylation potentials in the water column of lakes across Canada. *Sci. Total Env.* 368 (1), 111–125. <https://doi.org/10.1016/j.scitotenv.2005.09.042>.

Finn, R.D., Clements, J., Eddy, S.R., 2011. HMMER web server: interactive sequence similarity searching. *Nucleic Acids Res.* 39 (Web Server issue), W29–W37. <https://doi.org/10.1093/nar/gkr367>.

Fleming, E.J., Mack, E.E., Green, P.G., Nelson, D.C., 2006. Mercury methylation from unexpected sources: molybdate-inhibited freshwater sediments and an iron-reducing bacterium. *Appl. Env. Microbiol.* 72 (1), 457–464. <https://doi.org/10.1128/AEM.72.1.457-464.2006>.

Friedrich, J., Janssen, F., Aleynik, D., Bange, H.W., Boltacheva, N., Çagatay, M.N., Dale, A.W., Etiöpe, G., Erdem, Z., Geraga, M., Gilli, A., Gomoiu, M.T., Hall, P.O.J., Hansson, D., He, Y., Holtappels, M., Kirf, M.K., Kononets, M., Konovalov, S., Lichtschlag, A., Livingstone, D.M., Marinaro, G., Mazlumyan, S., Naeher, S., North, R.P., Papatheodorou, G., Pfannkuche, O., Prier, R., Rehder, G., Schubert, C.J., Soltwedel, T., Sommer, S., Stahl, H., Stanev, E.V., Teaca, A., Tengberg, A., Waldmann, C., Wehrli, B., Wenzhöfer, F., 2014. Investigating hypoxia in aquatic environments: diverse approaches to addressing a complex phenomenon. *Biogeosciences* 11 (4), 1215–1259. <https://doi.org/10.5194/bg-11-1215-2014>.

Gallorini, A., Loizeau, J.-L., 2021. Mercury methylation in oxic aquatic macro-environments: a review. *J. Limnol.* 80 (2). <https://doi.org/10.4081/jlimnol.2021.2007>.

Gallorini, A., Loizeau, J.-L., 2022. Lake snow as a mercury methylation micro-environment in the oxic water column of a deep peri-alpine lake. *Chemosphere* 299, 134306. <https://doi.org/10.1016/j.chemosphere.2022.134306>.

Gambardella, N., Costa, J., Martins, B.M., Folhas, D., Ribeiro, A.P., Hintelmann, H., Canário, J., Magalhães, C., 2025. The role of prokaryotic mercury methylators and demethylators in Canadian Arctic thermokarst lakes. *Sci. Rep.* 15 (1), 7173. <https://doi.org/10.1038/s41598-025-89438-7>.

Garner, R.E., Kraemer, S.A., Onana, V.E., Fradette, M., Varin, M.-P., Huot, Y., Walsh, D. A., 2023. A genome catalogue of lake bacterial diversity and its drivers at continental scale. *Nat. Microbiol.* 1–15. <https://doi.org/10.1038/s41564-023-01435-6>.

Garnier, S., Ross, N., Rudis, R., Camargo, P. A., Sciaiani, M., Scherer, C., 2024. viridis (Lite): colorblind Friendly Color Maps for R, R package version 0.6.5. <https://sjmgarnier.github.io/viridis/>.

Gascón Díez, E., Loizeau, J.-L., Cosio, C., Bouchet, S., Adatte, T., Amouroux, D., Bravo, A. G., 2016. Role of settling particles on mercury methylation in the oxic water column of freshwater systems. *Env. Sci. Technol.* 50 (21), 11672–11679. <https://doi.org/10.1021/acs.est.6b03260>.

Gilmour, C.C., Podar, M., Bullock, A.L., Graham, A.M., Brown, S.D., Somenahally, A.C., Johs, A., RAJr, Hurt, Bailey, K.L., Elias, D.A., 2013. Mercury methylation by novel microorganisms from new environments. *Env. Sci. Technol.* 47 (20), 11810–11820. <https://doi.org/10.1021/es403075t>.

Gionfriddo, C.M., Wymore, A.M., Jones, D.S., Wilpiszeski, R.L., Lynes, M.M., Christensen, G.A., Soren, A., Gilmour, C.C., Podar, M., Elias, D.A., 2020. An improved hgcAB primer set and direct high-throughput sequencing expand Hg-methylator diversity in nature. *Front. Microbiol.* 11. <https://doi.org/10.3389/fmicb.2020.541554>.

Gorokhova, E., Soerensen, A.L., Motwani, N.H., 2020. Mercury-methylating bacteria are associated with copepods: a proof-of-principle survey in the Baltic Sea. *PLOS ONE* 15 (3), e0230310. <https://doi.org/10.1371/journal.pone.0230310>.

Harrell Jr, F.E., Harrell Jr, M.F., 2019. Package 'hmsc'. *CRAN 2019*, 235–236, 2018.

Hintelmann, H., 2010. Organomercurials. Their formation and pathways in the environment. *Met. Ions Life Sci.* 7, 365–401. <https://doi.org/10.1039/BK9781847551771-00365>.

Hyatt, D., Chen, G.-L., LoCascio, P.F., Land, M.L., Larimer, F.W., Hauser, L.J., 2010. Prodigal: prokaryotic gene recognition and translation initiation site identification. *BMC Bioinform.* 11 (1), 119. <https://doi.org/10.1186/1471-2105-11-119>.

Jane, S.F., Hansen, G.J.A., Kraemer, B.M., Leavitt, P.R., Mincer, J.L., North, R.L., Pilla, R. M., Stetler, J.T., Williamson, C.E., Woolway, R.I., Arvola, L., Chandra, S., DeGasperi, C.L., Diemer, L., Dunalska, J., Erina, O., Flaim, G., Grossart, H.-P., Hambright, K.D., Hein, C., Hejzlar, J., Janus, L.L., Jenny, J.-P., Jones, J.R., Knoll, L. B., Leoni, B., Mackay, E., Matsuzaki, S.-I.S., McBride, C., Müller-Navarra, D.C., Paterson, A.M., Pierson, D., Rogora, M., Rusak, J.A., Sadro, S., Saulnier-Talbot, E., Schmid, M., Sommaruga, R., Thiery, W., Verburg, P., Weathers, K.C., Weyhenmeyer, G.A., Yokota, K., Rose, K.C., 2021. Widespread deoxygenation of temperate lakes. *Nature* 594 (7861), 66–70. <https://doi.org/10.1038/s41586-021-03550-y>.

Ji, X., Liu, C., Pan, G., 2020a. Interfacial oxygen nanobubbles reduce methylmercury production ability of sediments in eutrophic waters. *Ecotoxicol. Env. Saf.* 188, 109888. <https://doi.org/10.1016/j.ecoenv.2019.109888>.

Ji, X., Liu, C., Zhang, M., Yin, Y., Pan, G., 2020b. Mitigation of methylmercury production in eutrophic waters by interfacial oxygen nanobubbles. *Water Res.* 173, 115563. <https://doi.org/10.1016/j.watres.2020.115563>.

Jiang, Q., Sun, Y., Jeppesen, E., Smol, J.P., Scavia, D., Hecky, R.E., Mehner, T., Qin, Y., Tong, Y., Qin, B., Hambright, K.D., Jin, X., Li, J., Cai, K., Wu, Z., Liu, Y., 2025. Persistent inequities in global lake science. *Nat. Rev. Earth Environ.* 6, 629–631. <https://doi.org/10.1038/s43017-025-00722-6>.

Jones, D.S., Walker, G.M., Johnson, N.W., Mitchell, C.P.J., Coleman Wasik, J.K., Bailey, J.V., 2019. Molecular evidence for novel mercury methylating

microorganisms in sulfate-impacted lakes. *ISME J* 13 (7), 1659–1675. <https://doi.org/10.1038/s41396-019-0376-1>.

Jürgens, K., Taylor, G., 2018. Biogeochemistry and microbiology of oxygen-depleted water columns. *Microbial Ecology of the Oceans*.

Kallistova, A.Yu., Kosyakova, A.I., Rusanov, I.I., Kadnikov, V.V., Beletsky, A.V., Koval', D. D., Yusupov, S.K., Zekker, I., Pimenov, N.V., 2023. Methane production in a temperate freshwater lake during an intense cyanobacterial bloom. *Microbiology* 92 (5), 638–649. <https://doi.org/10.1134/S00261723601586>.

Langmead, B., Salzberg, S.L., 2012. Fast gapped-read alignment with Bowtie 2. *Nat Methods* 9 (4), 357–359. <https://doi.org/10.1038/nmeth.1923>.

Li, D., Liu, C.-M., Luo, R., Sadakane, K., Lam, T.-W., 2015. MEGAHT: an ultra-fast single-node solution for large and complex metagenomics assembly via succinct de Bruijn graph. *Bioinformatics* 31 (10), 1674–1676. <https://doi.org/10.1093/bioinformatics/btv033>.

Li, H., Handsaker, B., Wysoker, A., Fennell, T., Ruan, J., Homer, N., Marth, G., Abecasis, G., Durbin, R., 1000 Genome Project Data Processing Subgroup, 2009. The sequence alignment/map format and SAMTools. *Bioinformatics* 25 (16), 2078–2079. <https://doi.org/10.1093/bioinformatics/btp352>.

Liao, Y., Smyth, G.K., Shi, W., 2014. featureCounts: an efficient general purpose program for assigning sequence reads to genomic features. *Bioinformatics* 30 (7), 923–930. <https://doi.org/10.1093/bioinformatics/btt656>.

Lin, H., Ascher, D.B., Myung, Y., Lamborg, C.H., Hallam, S.J., Gionfriddo, C.M., Holt, K. E., Moreau, J.W., 2021. Mercury methylation by metabolically versatile and cosmopolitan marine bacteria. *ISME J* 15 (6), 1810–1825. <https://doi.org/10.1038/s41396-020-00889-4>.

Mason, R.P., Choi, A.L., Fitzgerald, W.F., Hammerschmidt, C.R., Lamborg, C.H., Soerensen, A.L., Sunderland, E.M., 2012. Mercury biogeochemical cycling in the ocean and policy implications. *Env. Res* 119, 101–117. <https://doi.org/10.1016/j.envres.2012.03.013>.

Matzen, F.A., Kodner, R.B., Armbrust, E.V., 2010. pplacer: linear time maximum-likelihood and bayesian phylogenetic placement of sequences onto a fixed reference tree. *BMC Bioinform.* 11 (1), 538. <https://doi.org/10.1186/1471-2105-11-538>.

McDaniel, E.A., Peterson, B.D., Stevens, S.L.R., Tran, P.Q., Anantharaman, K., McMahon, K.D., 2020. Expanded phylogenetic diversity and metabolic flexibility of mercury-methylating microorganisms. *mSystems* 5 (4). <https://doi.org/10.1128/mSystems.00299-20> e00299-20.

McMurdie, P.J., Holmes, S., 2013. phyloseq: an R package for reproducible interactive analysis and graphics of microbiome census data. *PLOS ONE* 8 (4), e61217. <https://doi.org/10.1371/journal.pone.0061217>.

Ogle, D., Ogle, M.D., 2017. Package 'fsa'. *Cran Repos* 1–206.

Oksanen, J., Blanchet, F.G., Kindt, R., Legendre, P., Minchin, P.R., O'hara, R.B., Oksanen, M.J., 2013. Package 'vegan'. *Community ecol. package version 2* (9), 1–295.

Parks, J.M., Jogs, A., Podar, M., Bridou, R., Hurt, R.A., Smith, S.D., Tomanicek, S.J., Qian, Y., Brown, S.D., Brandt, C.C., Palumbo, A.V., Smith, J.C., Wall, J.D., Elias, D. A., Liang, L., 2013. The genetic basis for bacterial mercury methylation. *Science* 339 (6125), 1332–1335. <https://doi.org/10.1126/science.1230667>.

Pedersen, T.L., 2023. *ggforce: accelerating ggplot2*, R package version 0.4.2. <https://CRAN.R-project.org/package=ggforce>.

Peterson, B.D., McDaniel, E.A., Schmidt, A.G., Lepak, R.F., Janssen, S.E., Tran, P.Q., Marick, R.A., Ogorek, J.M., DeWild, J.F., Krabbenhoft, D.P., McMahon, K.D., 2020. Mercury methylation genes identified across diverse Anaerobic microbial guilds in a eutrophic sulfate-enriched lake. *Env. Sci Technol* 54 (24), 15840–15851. <https://doi.org/10.1021/acs.est.0c05435>.

Peterson, B.D., Poulin, B.A., Krabbenhoft, D.P., Tate, M.T., Baldwin, A.K., Naymik, J., Gastelecutto, N., McMahon, K.D., 2023a. Metabolically diverse microorganisms mediate methylmercury formation under nitrate-reducing conditions in a dynamic hydroelectric reservoir. *ISME J* 17 (10), 1705–1718. <https://doi.org/10.1038/s41396-023-01482-1>.

Pirrone, N., Cinnirella, S., Feng, X., Finkelman, R.B., Friedli, H.R., Leaner, J., Mason, R., Mukherjee, A.B., Stracher, G.B., Streets, D.G., Telmer, K., 2010. Global mercury emissions to the atmosphere from anthropogenic and natural sources. *Atmos. Chem. Phys.* 10 (13), 5951–5964. <https://doi.org/10.5194/acp-10-5951-2010>.

Podar, M., Gilmour, C.C., Brandt, C.C., Soren, A., Brown, S.D., Crable, B.R., Palumbo, A. V., Somenahally, A.C., Elias, D.A., 2015. Global prevalence and distribution of genes and microorganisms involved in mercury methylation. *Sci Adv* 1 (9), e1500675. <https://doi.org/10.1126/sciadv.1500675>.

Pereira-Garcia, C., Bravo, A.G., Cosio, C., Gallorini, A., Leoni, S., Cassin, D., Guédron, S., Adatte, T., Cabrera-Brufau, M., Sánchez, O., Acinas, S.G., Amouroux, D., Zonta, R., Dominik, J., Loizeau, J.-L., 2025. Potential impact of tide-regulation barriers on the formation of methylmercury in the Venice Lagoon (Italy). *J. Hazard. Mater* 485, 136747. <https://doi.org/10.1016/j.jhazmat.2024.136747>.

Peterson, B.D., Poulin, B.A., Krabbenhoft, D.P., Tate, M.T., Baldwin, A.K., Naymik, J., Gastelecutto, N., McMahon, K.D., 2023b. Metabolically diverse microorganisms mediate methylmercury formation under nitrate-reducing conditions in a dynamic hydroelectric reservoir. *ISME J* 17 (10), 1705–1718. <https://doi.org/10.1038/s41396-023-01482-1>.

Rudis, B., Bichat, A., 2023. ggchicklet: create "chicklet" (rounded segmented column) charts, R package version 0.5.2. <https://github.com/hrbrmstr/ggchicklet>.

Sanseverino, I., Pretto, P., António, D.C., Lahm, A., Faccia, C., Loos, R., Skejo, H., Beghi, A., Pandolfi, F., Genoni, P., Lettieri, T., 2022. Metagenomics analysis to investigate the microbial communities and their functional profile during cyanobacterial blooms in Lake Varese. *Microb Ecol* 83 (4), 850–868. <https://doi.org/10.1007/s00248-021-01914-5>.

South, A., South, M.A., 2017. R package: rnaturalearth. World Map data from Natural Earth, version 0.1. 0. Available online. <https://cran.r-project.org/web/packages/rnaturalearth/rnaturalearth.pdf>, accessed on 12 November 2024.

Truong, D.T., Franzosa, E.A., Tickle, T.L., Scholz, M., Weingart, G., Pasolli, E., Tett, A., Huttenhower, C., Segata, N., 2015. MetaPhlAn2 for enhanced metagenomic taxonomic profiling. *Nat Methods* 12 (10), 902–903. <https://doi.org/10.1038/nmeth.3589>.

Vigneron, A., Cruaud, P., Aubé, J., Guyoneaud, R., Goñi-Urriza, M., 2021. Transcriptomic evidence for versatile metabolic activities of mercury cycling microorganisms in brackish microbial mats. *npj Biofilms Microbiomes* 7 (1), 83. <https://doi.org/10.1038/s41522-021-00255-y>.

Wickham, H., Vaughan, D., & Girlich, M. (2024). tidy: tidy messy data (Version 1.3. 1) [Computer software].

Wickham, H., Wickham, M.H., & RColorBrewer, I. (2016). Package 'scales'. R package version, 1(0).

Wickham, H. (2011). ggplot2. Wiley interdisciplinary reviews: computational statistics, 3 (2), 180–185.

Wei, T., Simko, V., 2021. R package 'corrplot': visualization of a correlation matrix (Version 0.95). Package Corrplot for R Software. Available from. <https://github.com/taiyun/corrplot>.

Woolway, R.I., Kraemer, B.M., Lenters, J.D., Merchant, C.J., O'Reilly, C.M., Sharma, S., 2020. Global lake responses to climate change. *Nat Rev Earth Env.* 1 (8), 388–403. <https://doi.org/10.1038/s43017-020-0067-5>.

Xing, P., Tao, Y., Luo, J., Wang, L., Li, B., Li, H., Wu, Q.L., 2020. Stratification of microbiomes during the holomictic period of Lake Fuxian, an alpine monomictic lake. *Limnol. Ocean.* 65 (S1), S134–S148. <https://doi.org/10.1002/lno.11346>.

Yang, Y., Li, Z., Song, W., Du, L., Ye, C., Zhao, B., Liu, W., Deng, D., Pan, Y., Lin, H., Cao, X., 2019. Metagenomic insights into the abundance and composition of resistance genes in aquatic environments: influence of stratification and geography. *Env. Int* 127, 371–380. <https://doi.org/10.1016/j.envint.2019.03.062>.

Zhang, Y., Shi, K., Woolway, R.I., Wang, X., Zhang, Y., 2025. Climate warming and heatwaves accelerate global lake deoxygenation. *Sci Adv* 11 (12), eadts5369. <https://doi.org/10.1126/sciadv.adt5369>.

Zhong, M., Barrenechea Angeles, I., More, K.D., Picard, M., Bertilsson, S., Bravo, A.G., Björn, E., Coolen, M.J.L., Capo, E., 2025. Climate-driven deoxygenation promoted potential mercury methylators in the past Black Sea water column. *Nat Water* 1–8. <https://doi.org/10.1038/s44221-025-00526-4>.

Zou, R., Wu, Z., Zhao, L., Elser, J.J., Yu, Y., Chen, Y., Liu, Y., 2020. Seasonal algal blooms support sediment release of phosphorus via positive feedback in a eutrophic lake: insights from a nutrient flux tracking modeling. *Ecol Model* 416, 108881. <https://doi.org/10.1016/j.ecolmodel.2019.108881>.